

# Coronagraphic mask design using Hermite functions

Manuel P. Cagigal,<sup>1,\*</sup> Vidal F. Canales,<sup>1</sup> Pedro J. Valle,<sup>1</sup> and José E. Oti<sup>2</sup>

<sup>1</sup>*Departamento de Física Aplicada, Universidad de Cantabria  
Los Castros S/N, 39005, Santander, Spain*

<sup>2</sup>*AOTEK S. COOP., B° San Andrés 19, Mondragón 20500, Spain  
\*perezcm@unican.es*

**Abstract:** We introduce a stellar coronagraph that uses a coronagraphic mask described by a Hermite function or a combination of them. It allows the detection of exoplanets providing both deep starlight extinction and high angular resolution. This angular resolution depends on the order of the Hermite function used. An analysis of the coronagraph performance is carried out for different even order masks. Numerical simulations of the ideal case, with no phase errors and perfect telescope pointing, show that on-axis starlight is reduced to very low intensity levels corresponding to a gain of at least 25 magnitudes ( $10^{-10}$  light intensity reduction). The coronagraphic throughput depends on the Hermite function or combination selected. The proposed mask series presents the same advantages of band limited masks along with the benefit of reducing the light diffracted by the mask border thanks to its particular shape. Nevertheless, for direct detection of Earth-like exoplanets it requires the use of adaptive optics facilities for compensating the perturbations introduced by the atmosphere and by the optical system.

©2009 Optical Society of America

OCIS codes: (100.2980) Image enhancement; (110.2970) Image detection systems.

---

## References and links

1. N. Woolf, and J. R. Angel, "Astronomical searches for Earth-like planets and signs of life," *Annu. Rev. Astron. Astrophys.* **36**(1), 507–537 (1998).
2. A. Beichman, N. J. Wolf, and C. A. Lindensmith, eds., *Terrestrial Planet Finder (TPF)* (JPL Publications 99–003, Jet Propulsion Laboratory, Pasadena, 1999).
3. O. Guyon, E. A. Pluzhnik, M. J. Kuchner, B. Collins, and S. T. Ridgway, "Theoretical limits on extrasolar planets detection with coronagraphs," *Astrophys. J. Suppl. Ser.* **167**(1), 81–99 (2006).
4. C. Aime, "Radon approach to shaped and apodized apertures for imaging exoplanets," *Astron. Astrophys.* **434**(2), 785–794 (2005).
5. O. Guyon, E. A. Pluzhnik, R. Galicher, F. Martinache, S. T. Ridgway, and R. A. Woodruff, "Exoplanet Imaging with a Phase-induced Amplitude Apodization Coronagraph. I. Principle," *Astrophys. J.* **622**(1), 744–758 (2005).
6. F. Roddier, and C. Roddier, "Stellar Coronagraph with phase mask," *Publ. Astron. Soc. Pac.* **109**, 815–820 (1997).
7. P. Baudoz, Y. Rabbia, and J. Gay, "Achromatic interfero coronagraphy," *Astron. Astrophys. Suppl. Ser.* **141**(2), 319–329 (2000).
8. D. Rouan, D. Riaud, A. Boccaletti, Y. Clénet, and A. Labeyrie, "The four-quadrant phase-mask coronagraph," *Publ. Astron. Soc. Pac.* **112**(777), 1479–1486 (2000).
9. G. Foo, D. M. Palacios, and G. A. Swartzlander, Jr., "Optical vortex coronagraph," *Opt. Lett.* **30**(24), 3308–3310 (2005).
10. M. J. Kuchner, and W. A. Traub, "A Coronagraph with a Band-limited Mask for Finding Terrestrial Planets," *Astrophys. J.* **570**(2), 900–908 (2002).
11. M. P. Cagigal, and V. F. Canales, "Exoplanet detection using a nulling interferometer," *Opt. Express* **9**(1), 36–41 (2001).
12. M. P. Cagigal, and V. F. Canales, "Speckle statistics in partially corrected wave fronts," *Opt. Lett.* **23**(14), 1072–1074 (1998).
13. V. F. Canales, and M. P. Cagigal, "Photon statistics in partially compensated wave fronts," *J. Opt. Soc. Am. A* **16**(10), 2550–2554 (1999).
14. A. Sivaramakrishnan, C. D. Koresko, R. B. Makidon, T. Berkefeld, and M. J. Kuchner, "Ground-based coronagraphy with high-order adaptive optics," *Astrophys. J.* **552**(1), 397–408 (2001).

15. J. E. Oti, V. F. Canales, and M. P. Cagigal, "Pure amplitude masks for exoplanet detection with the optical differentiation coronagraph," *Astrophys. J.* **662**(1), 738–743 (2007).
  16. P. J. Borde, and W. A. Traub, "High-contrast imaging from space: speckle nulling in a low-aberration regime," *Astrophys. J.* **638**(1), 488–498 (2006).
- 

## 1. Introduction

The list of discovered extrasolar planets orbiting Sun-like stars is continuously increasing since the first detection by indirect methods. The final goal of exoplanet detection is the acquisition of direct images of Earth-like planets around solar-type stars in order to perform spectroscopy of its atmosphere and look for habitable conditions and signs of life [1]. This is a formidable task because of the small star-planet angular separation and their large intensity contrast ratio. The more favorable intensity contrast ratio is in the mid-infrared,  $10^{-6}$  [2] whilst at visible wavelengths, this contrast ratio is more striking,  $10^{-9}$  -  $10^{-10}$ .

Two techniques have been proposed for achieving this extraordinary goal of direct detection: nulling interferometry and coronagraphy, but we will focus our attention on this last technique. Among coronagraphs, several types can be distinguished [3]. Some designs combine different beams from the pupil and, thus, resemble nulling interferometers. Other coronagraphs present pupil mask apodization, with amplitude [4] or with phase masks, as in the Phase-induced Amplitude Apodization Coronagraph (PIAAC) case [5], which offers the highest throughput and smallest working angle of any system with high useful throughput. Another relevant group of coronagraphs rely on masks at the intermediate image plane. Roddier & Roddier [6] proposed a phase mask covering the inner part of the star image. Further starlight extinction could be achieved by the Achromatic Interfero-Coronagraph (AIC) [7] or by the Four Quadrant Phase Mask coronagraph (FQ-PM) [8]. A focal plane vortex mask avoids the dead zones of this latter design [9]. The main problem of phase masks is that they perform poorly when the stellar angular size is considered [3]. Finally, Kuchner & Traub [10] introduced the use of band-limited masks (BLM). An interesting comparison of the performance of all these designs can be found in [3]. It must also be noted that we have considered unobstructed circular telescope pupils, but evolved coronagraphs use on purpose designed Lyot stops that match the residual pattern of the star due to the central obstruction or spiders.

Here we present a coronagraph based on a novel mask at the intermediate plane. The mask amplitude transmission is described by a Hermite function. It provides, as those already mentioned, perfect starlight extinction as well as both high angular resolution and high dynamic range. Under ideal conditions (non-aberrated wavefronts) our instrument is expected to permit direct detection of Earth-like exoplanets and to perform spectroscopy of its atmosphere. However, to take advantage of the coronagraph capabilities the use of space-based telescopes or extreme adaptive optics [11] is mandatory for reducing atmospheric distortions [12,13]. Simulations under ideal conditions have been carried out to show the proposed masks performances.

Hermite functions have been chosen because they are eigenfunctions of the Fourier transform and, as will be shown, this facilitates the designing of masks with a desired performance. In this work even Hermite functions are used, because they present the advantage of being amplitude-only functions. This implies that the masks to be built are not wavelength dependent. Nonetheless, the fabrication of the proposed masks will not be an easy task, especially the attaining of the correct behavior near the optical axis, but this problem is shared with most coronagraph mask designs.

The scheme of this paper is as follows: first the new coronagraph masks are described. Then, the performance attainable with these masks is analyzed. Finally, the most relevant conclusions are stood out.

## 2. Hermite Function masks

Let us consider the Hermite functions of variance  $\nu$ , which, conveniently rescaled, are eigenfunctions of the Fourier Transform, defined as:

$$M_n(x, v) = \frac{1}{\sqrt{n!2^n\sqrt{\pi}}} \exp\left(-\frac{x^2}{2v}\right) H_n(x) \quad (1)$$

where  $H_n(x)$  is the  $n$ -order Hermite polynomial given by

$$H_n(x) = (-1)^n e^{x^2} \frac{d}{dx^n} e^{-x^2} \quad (2)$$

Our instrument is a standard coronagraph in which the occulting mask is replaced by a mask whose amplitude-transmittance function is described by an even Hermite function. Note that  $x$  represents a real distance in the mask plane. The Fourier Transform (FT) of these masks fulfill:

$$\text{FT}[M_n(x, v)](u) = \sqrt{2\pi v} (2v-1)^{n/2} i^n M_n\left(\frac{2\pi v}{\sqrt{2v-1}}u, \frac{v}{2v-1}\right) \quad (3)$$

where  $u$  is the spatial frequency related to  $x$ . It can be seen that the FT of the mask is a scaled version of the original one. Later we will take advantage of this property.

To make this kind of mask it is only necessary to build an amplitude mask, while odd Hermite masks would use two complementary masks: an amplitude transmission mask proportional to  $|M_n(x, v)|$  with transmission ranging from 0 to 1, and a phase mask consisting of a phase step of  $-\pi/2$  for the negative valued coordinates and of  $+\pi/2$  for the positive ones so that the whole set provides an amplitude range from  $-1$  to  $1$ . Hermite masks are proposed for combining the best characteristics of different masks: small inner working angle (IWA) with a moderate sensitivity to stellar angular size. It must be noted that although the masks are not strictly band limited, they are almost band limited because there is a finite interval outside where the FT of the mask, which is again a Hermite function, has smaller values than any desired limit.

The contribution of the Hermite function mask (HFM), with respect to other finite size masks, is that there is no starlight diffracted by the mask outer border, thanks to the fact that the transmittance falls quickly down to zero, providing deeper starlight extinction. Another advantage of this kind of mask is that it allows a little pointing error since the mask transmittance can decrease quickly to zero in the axis surroundings ( $x = 0, y = 0$ ).

Now, we will describe the classical coronagraph following the notation proposed by Sivaramakrishnan [14]. We will follow the path of the electric field as it passes through the coronagraph depicted in Fig. 1. Let  $\tilde{A}(u)$  be the field amplitude at the coronagraph aperture. Then, the field at the image focal plane of the first lens (L1),  $A(x)$ , will be the Fourier Transform of  $\tilde{A}(u)$ . After the mask, described by the transmission function  $M(x)$ , we will get the product  $M(x)A(x)$ . This field, once transformed by the second lens (L2) becomes  $\tilde{M}(u) * \tilde{A}(u)$  (where  $*$  denotes convolution) that, once multiplied by the Lyot stop transmission function  $\tilde{L}(u)$ , produces the throughput field  $\tilde{L}(u)[\tilde{M}(u) * \tilde{A}(u)]$ . A third lens L3 performs the last Fourier Transform to provide the final image  $L(x)[M(x)A(x)]$  which is detected by a scientific camera. This final image must be zero for an on-axis object. However, a tilted source produces a tilted field  $\tilde{A}'(u)$  so that the Lyot stop is unable to block the light coming from this source and the product  $\tilde{L}(u)[\tilde{M}(u) * \tilde{A}'(u)]$  will be no longer zero. Therefore, the light coming from the centered star is removed allowing the search for a potential faint object in the circumstellar environment.

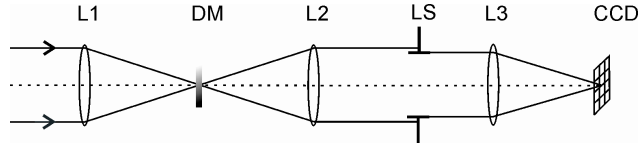


Fig. 1. Set-up of the proposed stellar coronagraph. It is composed of 3 lenses, L1, L2 and L3, the Lyot stop, LS, the mask, HFM, placed at the common focal plane of L1 and L2, and an imaging system like a CCD camera.

To ensure the energy cancellation, it is enough a null convolution product  $\tilde{M}(u) * \tilde{A}(u)$  inside the Lyot stop. There are several kind of masks satisfying this condition as, for example, the already mentioned FQ-PM, the BLM and the ODC mask. However, the success of a coronagraph depends on how it performs in other aspects as will be analyzed later on.

As we have seen, a mask  $M(x)$  has to be selected to force the convolution product  $\tilde{M}(u) * \tilde{A}(u)$  to be zero inside the Lyot stop. We propose to use Hermite functions since they have the advantage of being invariant under Fourier Transform, that is, the shape of  $\tilde{M}(u)$  will be the same of  $M(x)$  except for scale and normalization factors. Then, a proper combination of even Hermite functions masks,  $M_n(x, v)$ , ensures that the corresponding Fourier Transformed function retains the original shape, which convolved with the ideal star field results negligible in the inner part of the Lyot pupil. Thanks to the linearity of the Fourier Transform and of the convolution product, a combination of Hermite functions with different variances can also be successfully used:

$$M_c(x) = \sum_k a_k M_{n_k}(x, v_k) \quad n_k \text{ even} \quad (4)$$

At this point, a further description of the mask should be made. The mask proposed  $M_n(x; v)$  is an amplitude mask whose amplitude is described by an even Hermite function as shown in Eq. (1). In particular, the second-order even Hermite function that cancels the convolution product inside the Lyot stop is

$$MC_2(x, v) = M_2(x, v) + \frac{1}{\sqrt{2}} M_0(x, v) = \frac{1}{\sqrt{2!2^2\sqrt{\pi}}} \exp\left(-\frac{x^2}{2v}\right) [H_2(x) + 2H_0(x)] \quad (5)$$

Higher order masks can be calculated analogously. In particular, note that  $MC_2(x, v)$  is the differentiation mask in the Optical Differentiation Coronagraph (ODC) [15]. In addition, a Hermite function can be considered as a combination of differentiation masks of different orders.

### 3. HFM performance

We check the performance of our coronagraphic masks by means of numerical simulations following the standard procedure described in previous papers [15]. To analyze the behaviour of the HFM coronagraph a series of masks has been selected. Figure 2 shows the mask profiles for  $MC_4$ ,  $MC_6$ ,  $MC_8$  (normalized to a maximum value of 1) and a combination of these normalized profiles:  $M_C = 0.774 (MC_4 + 0.5 MC_6 + 0.95 MC_8)$ . Taking into account that all the HFM provide deep extinction of the star light, the mask analysis must be focused on the comparison of the inner working angle (IWA) and throughput, which are coupled because the IWA is usually defined as the minimum angular distance at which the throughput for the planet is half of the maximal throughput. The IWA represents the minimum angular separation of an exoplanet from its parent star to be detectable. Small IWA implies that exoplanets could be detected in even more distant stars, thus, increasing the number of surveyed stars. In a standard coronagraph, the IWA lies between  $2\lambda/D$  and  $4\lambda/D$ .

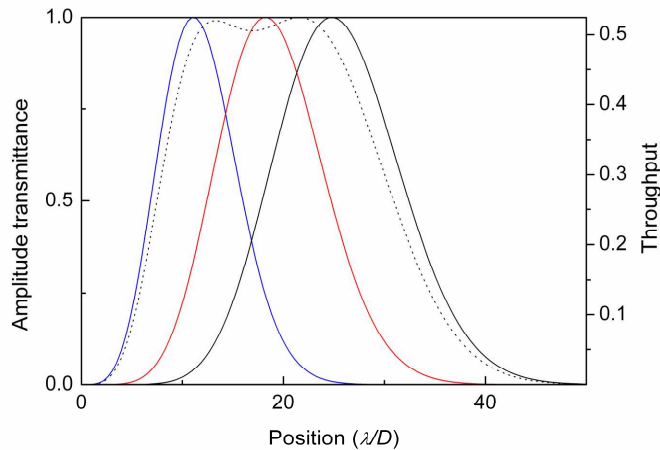


Fig. 2. Design of the HFM required in our instrument. a) Amplitude transmittance of the  $MC_4$  mask (blue curve),  $MC_6$  mask (red curve),  $MC_8$  (black solid curve) and  $MC$  (dashed curve).

It can be observed that the throughput for on-axis object is zero in all cases. For  $MC_4$  the throughput increases very quickly, it has a small IWA. For  $MC_6$  and  $MC_8$  the throughput increases slower than for  $MC_4$ , this means that it is more difficult to detect objects slightly out of axis using  $MC_6$  and  $MC_8$  than using  $MC_4$ . However,  $MC_8$  presents the advantage of high throughput for objects which are far from the on-axis star. It can also be seen that a convenient combination of Hermite functions like  $M_C$  presents a high throughput in the nearest proximities of the parent star but it also retains high values even for far objects. Although this is only an example, it is helpful to show that this method allows the design of masks working properly for the whole range of useful angular distances. Masks have a radius in the  $x$  direction of about  $100\lambda/D$  and the gaussian profile has a variance of  $\nu = 10, 18$  and  $25$  in units of  $(\lambda/D)^2$  for  $MC_4, MC_6$  and  $MC_8$  respectively.

Simulations have been carried out considering a circular Lyot stop with radius larger than the 80% of the entrance pupil radius. The Lyot stop could be optimized to match the shape of the image at the pupil to improve the exoplanet light throughput without losses in starlight extinction. The optimum Lyot's shape resembles that described by Kuchner & Traub [10].

In Fig. 3 we present the extinction results of our instrument for the perfect wavefront case. Simulations show that  $MC_4$  mask does not produce more light extinction than higher order masks, and it yields a similar extinction to  $M_C$  mask, although detection of faint objects in the stellar surroundings can be performed in all cases for an ideal star. Other significant aspect to be taken into account is the throughput values for large angular distances. While masks  $MC_6$  and  $MC_8$  increase the angular distance for which the throughput remains high, they present a large IWA. However, the  $M_C$  mask shows both small IWA and high throughput values for large angular distances together with a perfect light extinction for ideal on-axis objects. It must be noted that an actual star has a finite size, and then, a mask which presents 2nd-order transmission at the origin, would not reject enough starlight for planet detection. For that reason our different masks present at least 4th-order transmission at the origin, at the expense of IWA.

It must also be noted that the masks' high transmission regions coincide with the area in the image plane where deformable mirrors remove scattered light [16]. Outside this region, our masks suppress additional star light and thus they may be able to reduce the dynamic range of detectors required for observations. This could help to prevent saturation and related read-out issues.

Although the  $M_C$  mask is a specific combination of Hermite functions, many other masks can be designed as a function of the performances required for the coronagraph. As an

example, the masks series consisting of linear combinations of first order Hermite functions can be easily described in base of the previous analysis concerning to optical differentiation instruments [15] and they perform as it is required for coronagraphic starlight extinction in ideal conditions. Nonetheless, the latter masks present some disadvantages when aberrations are considered or when the actual star size is taken into account. Then, our method allows the design of a mask with lower aberration sensitivity and the desired transmission at the origin. In such conditions, the throughput and IWA will obviously deteriorate, but the key point is that the method enables the search for the adequate mask in different conditions.

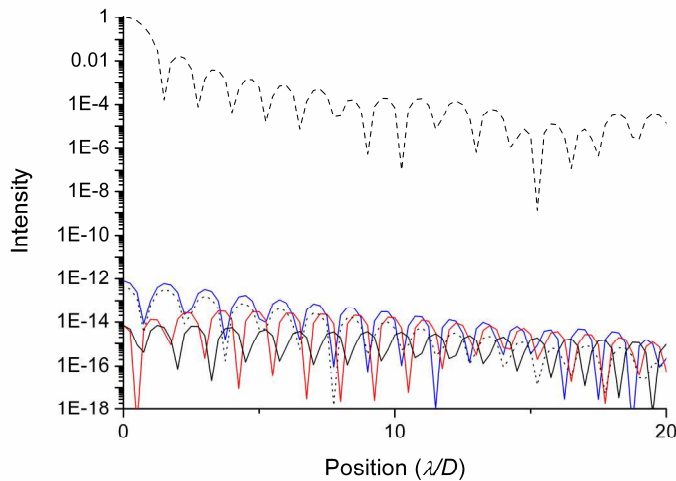


Fig. 3. Radial intensity profile obtained for the mask  $MC_4$  (dotted curve),  $MC_6$  (dashed-dotted curve),  $MC_8$  (solid curve) and  $M_C$  (dashed curve) in the perfect wavefront case. For comparison, the dashed-dotted-dotted curve shows the no-filter profile (with the stop).

#### 4. Conclusions

We have described a novel coronagraph which uses a mask whose transmittance profile is given by Hermite functions or a combination of them. This kind of masks provides deep on-axis starlight extinction, small IWA and high throughput. We have analyzed even masks, which are composed of an amplitude transmittance filter. Numerical simulations prove that star extinctions of up to 37 magnitudes ( $10^{-15}$  intensity reduction) are achieved for a perfect instrumented with no phase distortion. Besides, different even Hermite polynomials present different behaviors. Low order Hermite functions present small IWA but the throughput decreases quickly for objects at angular distances of a few  $\lambda/D$ . Large order Hermite functions have the advantage of presenting large throughput even for far objects but they have a large IWA. However, convenient combinations of functions can joint the advantages of low and large order function at the same time, as it is shown in the particular mask  $M_C$ .

The main contribution of this paper is the introduction of a masks series which presents the same advantages as band limited masks but with a finite size, what reduces the mask border diffracted light. These masks could be suitable to detect and even, under convenient distortion compensation, to perform spectroscopy of the elusive Earth-like exoplanets.

#### Acknowledgements

This research was supported by Ministerio de Educacion y Ciencia grant AYA 2007-67287